Journal of Nuclear Medicine, published on April 13, 2020 as doi:10.2967/jnumed.119.241356

Folate Receptor β Targeted PET Imaging of Macrophages in Autoimmune Myocarditis

Arghavan Jahandideh, MSc,[1,2] Sauli Uotila, MD,[1] Mia Ståhle, MSc,[1] Jenni Virta, MSc,[1] Xiang-Guo Li, PhD,[1,3] Ville Kytö, MD, PhD,[4] Päivi Marjamäki, PhD,[1] Heidi Liljenbäck, MSc,[1,5] Pekka Taimen, MD, PhD,[6] Vesa Oikonen, MSc,[1] Jukka Lehtonen, MD, PhD,[7] Mikko I. Mäyränpää, MD, PhD,[8] Qingshou Chen, PhD,[9] Philip S. Low, PhD,[9] Juhani Knuuti, MD, PhD,[1,2] Anne Roivainen, PhD,[1,2,5] and Antti Saraste, MD, PhD[1,2,4 *]

[1]Turku PET Centre, University of Turku, Turku, Finland.

[2]Turku PET Centre, Turku University Hospital, Turku, Finland.

[3]Turku PET Centre, Åbo Akademi University, Turku, Finland.

[4]Heart Center, Turku University Hospital and University of Turku, Turku, Finland.

[5]Turku Center for Disease Modeling, University of Turku, Turku, Finland.

[6]Institute of Biomedicine, University of Turku and Department of Pathology, Turku University Hospital, Turku, Finland.

[7]Heart and Lung Center, Helsinki University and Helsinki University Hospital, Helsinki, Finland.

[8]Pathology, Helsinki University and Helsinki University Hospital, Helsinki, Finland.

Department of Chemistry, Purdue University, West Lafayette, Indiana, USA.

[*]Corresponding author.

Short title: **Folate Receptor Imaging in Myocarditis**

Corresponding author: Antti Saraste, Heart Center, Turku University Hospital, Hämeentie 11, FI-20520 Turku, Finland. Email: antti.saraste@utu.fi, Tel: +35823130083

First author: Arghavan Jahandideh (PhD student), Turku PET Centre, University of Turku, Kiinamyllynkatu 4–8, FI-20520 Turku, Finland. Email: Arghavan.jahandideh@utu.fi, Tel: +358400214721

The total word count of the manuscript: 5000

This study was financially supported by grants from the Academy of Finland, Business Finland, Jane and Aatos Erkko Foundation, Finnish Foundation for Cardiovascular Research, and Sigrid Jusélius Foundation.

ABSTRACT

Rationale– Currently available imaging techniques have limited specificity for the detection of active myocardial inflammation. Aluminum fluoride-18-labeled 1,4,7-triazacyclononane-*N,N′,N″*-triacetic acid conjugated folate (^{18}F-FOL) is a positron emission tomography (PET) tracer targeting folate receptor β (FR-β) that is expressed on activated macrophages at sites of inflammation. We evaluated ^{18}F-FOL PET for the detection of myocardial inflammation in rats with autoimmune myocarditis and studied expression of FR-β in human cardiac sarcoidosis specimens.

Methods– Myocarditis was induced by immunizing rats (*n* = 18) with porcine cardiac myosin in complete Freund's adjuvant. Control rats (*n* = 6) were injected with Freund's adjuvant alone. ^{18}F-FOL was intravenously injected followed by imaging with a small animal PET/computed tomography (CT) scanner and autoradiography. Contrast-enhanced high-resolution CT or 2-deoxy-2-^{18}F-fluoro-*D*-glucose (^{18}F-FDG) PET images were used for co-registration. Rat tissue sections and myocardial autopsy samples of 6 patients with cardiac sarcoidosis were studied for macrophages and FR-β.

Results– The myocardium of 10 out of 18 immunized rats showed focal macrophage-rich inflammatory lesions with FR-β expression occurring mainly in M1-polarized macrophages. PET images showed focal myocardial ^{18}F-FOL uptake co-localizing with inflammatory lesions (SUV_{mean}, 2.1 ± 1.1), whereas uptake in the remote myocardium of immunized rats and controls was low (SUV_{mean}, 0.4 ± 0.2 and 0.4 ± 0.1, respectively; $P < 0.01$). *Ex vivo* autoradiography of tissue sections confirmed uptake of ^{18}F-FOL in myocardial inflammatory lesions. Uptake of ^{18}F-FOL to inflamed myocardium was efficiently blocked by a non-labeled FR-β ligand folate glucosamine *in vivo*. The myocardium of patients with cardiac sarcoidosis showed many FR-β-positive macrophages in inflammatory lesions.

Conclusion– In a rat model of autoimmune myocarditis, ^{18}F-FOL shows specific uptake in inflamed myocardium containing macrophages expressing FR-β, which were also present in human cardiac sarcoid lesions. Imaging of FR-β expression is a potential approach for the detection of active myocardial inflammation.

Key Words: folate receptor; positron emission tomography; myocarditis; experimental autoimmune myocarditis

INTRODUCTION

Myocarditis is an inflammatory disease of the heart characterized by myocardial inflammatory lesions and myocyte necrosis resulting from infection, cardiotoxic agents, or autoimmune diseases such as sarcoidosis. The clinical sequelae of myocarditis include conduction disturbances, ventricular arrhythmias, and inflammatory cardiomyopathy defined as myocarditis associated with cardiac dysfunction (*1*).

Diagnosis of myocarditis is challenging because of its wide clinical spectrum and nonspecific presentation. Endomyocardial biopsy is the gold standard for diagnosing myocarditis, but it has low sensitivity because of the focal nature of the disease (*2*). Thus, advanced non-invasive cardiac imaging, including cardiac magnetic resonance (CMR) and positron emission tomography/computed tomography (PET/CT) with 2-deoxy-2-^{18}F-fluoro-*D*-glucose (^{18}F-FDG), plays an important role in defining myocardial abnormalities (*2,3*).

Although ^{18}F-FDG PET/CT has shown high accuracy for the detection of cardiac inflammation and provides prognostic information (*4,5*), incomplete suppression of physiological myocardial ^{18}F-FDG uptake may impair its diagnostic accuracy (*6*). Therefore, more specific tracers for the detection of myocarditis on PET have recently been investigated (*7-12*).

Folate receptor β (FR-β) is a glycosylphosphatidylinositol-anchored membrane protein expressed on activated macrophages (*13*). Expression of FR-β has been found in many inflammatory diseases, including rheumatoid arthritis, Crohn's disease, ulcerative colitis, pulmonary disease, interstitial pneumonia, systemic lupus erythematosus, psoriasis, scleroderma, sarcoidosis, atherosclerosis, and myocardial infarction (*13-16*). Radiolabeled folate derivatives have been used to assess FR-β-positive activated macrophages at the site of inflammation, thereby suggesting FR-β as a potential target for diagnosis of inflammatory diseases (*13,15*). However, the feasibility of FR-β targeted imaging has not been studied in myocarditis.

We evaluated the feasibility of the recently developed FR-β targeting radiotracer aluminum fluoride-18-labeled 1,4,7-triazacyclononane-*N,N′,N″*-triacetic acid conjugated folate (^{18}F-FOL) (*15*) for PET imaging of myocardial inflammation in a rat model of autoimmune myocarditis. Myocarditis was induced by

immunization of rats with cardiac myosin in complete Freund's adjuvant. Myocardial uptake of ^{18}F-FOL was evaluated using small animal PET/CT imaging and *ex vivo* autoradiography. Expression of FR-β in myocardial inflammatory lesions was studied in rat hearts and in human cardiac sarcoidosis specimens.

METHODS

Animal Model and Study Protocol

Autoimmune myocarditis was induced as previously described (*17,18*). Briefly, male Lewis rats received subcutaneous injections of 5 mg/mL pig cardiac myosin (M0531; Sigma Aldrich) in an equal volume of complete Freund's adjuvant supplemented with 1 mg/mL *mycobacterium tuberculosis* (F5881; Sigma Aldrich), with two injections being given 7 days apart, either into the footpad or the hock of the left foot. To enhance immunization after the hock injection, the rats also received an intraperitoneal injection of 250 ng/mL pertussis toxin (P2980; Sigma Aldrich). Control rats were injected with the adjuvant alone. All procedures were performed under isoflurane anesthesia, with buprenorphine (0.03 mg/kg) being administered for analgesia two times/day for 2 days after immunization. A flow diagram of the study protocol and numbers of rats is shown in Fig. 1.

On day 21 after the first immunization, the rats underwent PET imaging with ^{18}F-FOL. Either contrast-enhanced CT or ^{18}F-FDG PET imaging was performed for localization of the myocardium. Following PET imaging, the rats were euthanized at 100 min after injection of ^{18}F-FOL, blood was drawn by cardiac puncture, and various organs including the heart were excised, weighed, and measured for radioactivity using a gamma counter (Triathler 3"; Hidex) for analysis of tracer biodistribution (*15*). The left ventricle (LV) was prepared and either embedded in optimal cutting temperature compound and frozen, or fixed in 10% formaldehyde and embedded in paraffin. The LVs were cut into serial transverse 20 μm and 8 μm cryosections, or 4 μm paraffin-embedded sections at 1 mm intervals from base to apex for autoradiography, histology, and immunostainings.

All animal experiments were approved by the national Animal Experiment Board in Finland and the Regional State Administrative Agency for Southern Finland, and were conducted in accordance with the relevant European Union directive.

Human Tissue Samples

Myocardial samples from five patients who died of cardiac sarcoidosis and one heart explanted due to sarcoidosis described earlier (*19*) were cut into serial 4 μm paraffin sections. Sections were immunohistochemically stained with an anti-CD68 antibody to detect macrophages and with an anti-FR-β antibody to study localization of FR-β. Double immunofluorescence staining was performed with an anti-CD68 antibody and with an anti-FR-β antibody (*20*). The use of human tissues was done in accordance with Finnish law, the principles of Declaration of Helsinki, and was approved by The National Authority for Medicolegal Affairs and the National Institute for Health and Welfare (*19*).

Radiotracer

^{18}F-FOL was prepared according to previously described procedures (*15*). The total radiosynthesis time of ^{18}F-FOL was 75–88 min starting from the end of bombardment. The radiochemical purity was >95% and the molar activity was 34 ± 9.3 GBq/μmol. The radiochemical yields (decay-corrected) were 57% ± 9.2%. *In vivo* stability of ^{18}F-FOL was studied as previously described (*15*) in venous blood obtained at 80 min after tracer injection from three controls and four immunized rats. The fraction of radioactivity related to intact tracer in plasma was 91% ± 2.3%.

***In Vivo* PET/CT Imaging**

^{18}F-FOL *in vivo* imaging was performed in isoflurane-anesthetized rats using a small animal PET/CT device (Inveon Multimodality; Siemens Medical Solutions) as previously described (*21,22*). The rats were injected with 50 ± 1.5 MBq ^{18}F-FOL via the tail vein. Either a 60 min dynamic PET acquisition (6 × 10 s, 4 × 60 s, 5 × 300 s, and 3 × 600 s frames) or a 10 min static PET acquisition starting at 30 min post-injection was performed.

To visualize myocardium, a 40 min static ^{18}F-FDG (50 ± 2.6 MBq) PET acquisition starting at 20 min post-injection was performed the day before the ^{18}F-FOL study. In addition, 300 µL intravascular iodinated contrast agent (eXia™ 160XL; Binitio Biomedical Inc.) was injected intravenously, and high-resolution CT imaging was performed immediately after the ^{18}F-FOL PET as described earlier (*21*).

Regions of interest of uniform size were defined in the ^{18}F-FOL images co-registered with CT or ^{18}F-FDG images using Carimas 2.9 software (Turku PET Centre, Turku, Finland) (*21*). Regions of interest were defined at the LV myocardium with or without visually increased ^{18}F-FOL uptake and the mean standardized uptake value (SUV_{mean}) was compared between histologically inflamed and non-inflamed myocardial regions defined by consensus of 2 readers who were blinded to other results. Additional regions of interest were drawn in the liver, lung, kidney, foreleg muscle, inferior vena cava, and LV (blood radioactivity). Decay-corrected time-activity curves were determined in rats with dynamic datasets. To estimate the tracer uptake kinetics, Logan, Patlak, and compartmental modeling were performed, and parametric images were obtained as previously described (*21,22*).

Ex Vivo Autoradiography, Histology and Immunostainings

To confirm uptake of ^{18}F-FOL in the myocardium, 20 µm cryosections were studied using digital autoradiography as previously described (*21,22*). The results are expressed as average photo-stimulated luminescence per square millimeter (PSL/mm^2) in multiple regions of interest drawn in the histologically inflamed and non-inflamed myocardium. For general histology, 20 µm cryosections were stained with hematoxylin and eosin. For immunohistochemistry, adjacent serial 4 µm paraffin sections were stained with an anti-FR-β antibody, an anti-CD3 antibody to detect lymphocytes, and an anti-CD68 antibody to detect macrophages. Additionally, an anti-iNOS antibody and an anti-CD206 antibody were used to detect pro-inflammatory (M1-polarized) and anti-inflammatory (M2-polarized) macrophages, respectively. To study the co-localization of FR-β with macrophage subsets, double immunofluorescence stainings were performed on cryosections. The cryosections were stained with biotinylated anti-FR-β (*20*) antibody detected with Streptavidin Alexa Fluor™ 488 conjugate followed by staining with either anti-CD68, anti-iNOS, or anti-CD206 antibody (Supplemental Table 1).

Effect of Folate Glucosamine on ^{18}F-FOL Uptake

To study the specificity of ^{18}F-FOL uptake, an *in vivo* blocking study was performed with co-injection of a 100-fold excess of FR-β ligand folate glucosamine ($C_{25}H_{30}N_8O_{10}$; 100 µL) 10 min prior to ^{18}F-FOL injection (Fig. 1). To further evaluate the specificity of the tracer, *in vitro* binding of ^{18}F-FOL in myocardial tissue sections from 3 immunized rats was studied in the presence or absence of a 100-fold excess of folate glucosamine as described earlier (*14*).

Statistical Analysis

Data are presented as mean ± standard deviation (SD). Paired or non-paired Student's *t*-test was applied to compare normally distributed data. GraphPad Prism 6 was used for the statistical analysis, and the threshold for statistical significance was set at $P<0.05$.

RESULTS

FR-β in Rat Autoimmune Myocarditis

Histological analysis of the rat hearts revealed focal cardiac inflammatory lesions in ten (56%) out of 18 immunized rats (six with hock injections and four with footpad injections), whereas no lesions were identified in the six control rats (Fig. 2).

The inflammatory lesions were mainly present close to the epicardium and showed myocyte necrosis and dense inflammatory cell infiltration. CD68-positive macrophages were the predominant cell type in the lesions and consisted of both M1- and M2-polarized macrophages. CD3-positive lymphocytes were present to a lesser extent. In immunized rats, the myocardium outside the inflammatory lesions appeared microscopically normal, and CD68 staining was virtually negative. Immunohistochemistry showed abundant FR-β-positive cells in the lesions, but not in the myocardium outside the lesions (Fig. 2).

Double immunofluorescence staining of inflamed myocardial lesions in the rats revealed co-localization of FR-β with CD68-positive macrophages, which were mainly M1-polarized (Fig. 3).

FR-β in Cardiac Sarcoidosis

Tissue samples of all patients with cardiac sarcoidosis showed FR-β expression in the inflammatory lesions that co-localized with CD68-positive macrophages (Fig. 4).

***In Vivo* PET/CT Imaging of FR-β**

In vivo imaging demonstrated clearly visible focal ^{18}F-FOL uptake in the LV myocardium in all rats with histologically proven inflammatory lesions (n = 7) in this subgroup, whereas there was no myocardial tracer uptake in any of the immunized rats without histological inflammation (n = 8) or in the control rats (n = 6; Fig. 5). Comparisons with histology indicated that ^{18}F-FOL uptake was co-localized with myocardial inflammatory lesions, whereas non-inflamed myocardium showed very low radioactivity. In total, there were 15 histologically verified separate inflammatory lesions in the seven rats with myocarditis that all showed increased ^{18}F-FOL uptake.

Time-activity curves in rats with inflamed lesions showed that ^{18}F-FOL radioactivity was rapidly cleared from the blood, whereas uptake in myocardial inflammatory lesions and most other tissues remained constant from 20 min post-injection (Fig. 6). The highest uptake was observed in the kidneys (SUV_{mean} 10.1 ± 4.5) consistent with elimination via the urinary system (Fig. 6).

Fig. 6 shows myocardial ^{18}F-FOL uptake in PET images at 30–40 min after injection. ^{18}F-FOL uptake in the inflammatory lesions was higher than uptake in the non-inflamed myocardium of immunized rats (SUV_{mean} 2.1 ± 1.1 vs. 0.4 ± 0.2; P = 0.004), with the ratio of ^{18}F-FOL uptake between inflammatory lesions and remote myocardium being around 5:1. The myocardial uptake in non-immunized controls (SUV_{mean} 0.4 ± 0.1) was similar to the non-inflamed myocardium of immunized rats (P = 0.4) and lower than in inflammatory lesions (P = 0.003). Tissues adjacent to the heart showed lower uptake than inflammatory lesions, with a SUV_{mean} of 0.3 ± 0.1 in LV blood, 0.3 ± 0.1 in lungs, and 1.2 ± 0.4 in liver.

Among the various kinetic models evaluated, the Logan model showed the best fit to the data (Supplemental Fig. 1A and 1B, Supplemental Table 2). Logan plots and parametric images of distribution volume (DV) were consistent with ^{18}F-FOL uptake in the inflamed myocardium (Supplemental Fig. 1A and 1C). The DV of ^{18}F-FOL was significantly higher in the inflamed than non-inflamed myocardium (DV, 4.0 ± 1.7 vs. 0.7 ± 0.2; P = 0.004) or the myocardium of control rats (DV, 0.8 ± 0.2; P = 0.003; Fig. 6). SUV_{mean} of ^{18}F-FOL at 30−40 min post-injection correlated well with DV (Supplemental Fig. 2).

Ex Vivo Autoradiography and Biodistribution

Autoradiography showed high uptake of ^{18}F-FOL in the inflammatory lesions of immunized rats, but low uptake in the non-inflamed myocardium of immunized rats and the myocardium of control rats (Fig. 7A). The average uptake of ^{18}F-FOL in inflammatory lesions (470 ± 180 PSL/mm^2; n = 7) was 7.8 ± 1.4 folds higher than in the non-inflamed myocardium of immunized rats (67 ± 43 PSL/mm^2; P = 0.0005; n = 7). The myocardium of control rats showed low activity (39 ± 15 PSL/mm^2; P = 0.0002 vs. inflamed lesions; P = 0.19 vs. non-inflamed myocardium of immunized rats; n = 6; Fig. 7B). Biodistribution of ^{18}F-FOL is presented in Supplemental Table 3.

Effect of Folate Glucosamine on ^{18}F-FOL Uptake

In vivo blocking of ^{18}F-FOL with a 100-fold excess of folate glucosamine in three immunized rats resulted in 77% lower ^{18}F-FOL uptake in inflammatory lesions than in rats injected with ^{18}F-FOL only (SUV_{mean} 0.6 ± 0.1 vs. 2.9 ± 0.4; P = 0.02; Fig. 7A). Folate glucosamine also effectively reduced *in vitro* binding of ^{18}F-FOL in inflamed myocardium in tissue sections (143 ± 27 vs. 2.4 ± 1.5 PSL/mm^2; P<0.0001; n = 3, Supplemental Fig. 3).

DISCUSSION

We demonstrate that ^{18}F-FOL shows specific uptake in inflamed myocardium in rats with autoimmune myocarditis. ^{18}F-FOL PET, as well as *ex vivo* autoradiography, showed high target-to-background ratios between inflamed lesions and non-inflamed myocardium. In the rat model, inflammatory lesions showed high densities of macrophages, particularly M1-polarized macrophages expressing FR-β. Furthermore,

macrophages in pathological specimens of human cardiac sarcoid lesions were shown to express FR-β. Imaging of FR-β expression in inflamed myocardium by ^{18}F-FOL PET is a novel approach for the non-invasive assessment of myocarditis.

The rat model of autoimmune myocarditis is a well-established experimental model of myocarditis with similarities to the human giant cell myocarditis leading to inflammatory cardiomyopathy (*17,23,24*). Although the exact mechanism underlying myocyte injury in autoimmune myocarditis is not fully understood, the disease process is thought to be initiated by autoreactive T-cells and macrophages (*17*). We studied rats at 21 days after their first immunization because the peak in inflammation in this model occurs at that time, as shown previously by histology and ^{18}F-FDG PET imaging (*24,25*). Focal myocardial inflammatory lesions characterized by myocyte destruction as well as by a high prevalence of macrophages (both M1- and M2-polarized) and CD3-positive lymphocytes are typical histological findings in this model (*23,24*). We expand on previous studies by providing evidence that FR-β is expressed and co-localized with M1-polarized macrophages in the rat model of myocarditis. Furthermore, we demonstrate that macrophages in human cardiac sarcoid lesions express FR-β.

Consistent with previous studies (*15*), our study indicates that ^{18}F-FOL shows specific uptake in FR-β-positive macrophages and favourable kinetics for *in vivo* imaging of inflammation. We demonstrated that ^{18}F-FOL PET is a potential approach for imaging myocarditis providing high target-to-background ratio. Other approaches, including ^{11}C-methionine-PET (*7*), 18-kDa translocator protein (TSPO)-targeting PET (*11*), fluorine-19-based CMR (*26)*, and ^{68}Ga-NOTA-MSA (mannosylated human serum albumin) PET (*27*), have also shown promising results for the detection of autoimmune myocarditis. Compared with anatomical imaging modalities, molecular imaging has the advantage of more specifically targeting sites of active inflammation. Although direct comparisons between different tracers are not possible, ^{18}F-FOL showed an at least comparable contrast between inflamed and non-inflamed myocardium to that previously described for ^{18}F-FDG (3.4 ± 0.7) or ^{11}C-methionine (2.1 ± 0.2) in the same model (*7*).

Kinetic modelling using graphical Patlak analysis supports the concept of irreversible ^{18}F-FOL uptake in inflamed myocardium, which is consistent with a previous study showing internalization of folate conjugates into endosomes (*28*). However, the Logan plot showed a better fit to the data, indicating that ^{18}F-FOL uptake may be partly reversible. The observed reversible component might be due to incomplete internalization of the ^{18}F-FOL, but this remains to be studied.

There are some limitations to our study. We were unable to directly compare uptake of ^{18}F-FDG and ^{18}F-FOL in inflamed myocardium due to physiological myocardial ^{18}F-FDG uptake. While our results indicate that FR-β is a potential marker of active myocardial inflammation in both the rat model and human cardiac sarcoidosis, its role in the pathogenesis of myocarditis remains to be studied. Assessing ^{18}F-FOL uptake in response to therapy remains to be evaluated in models with a reproducible disease intensity. Notably, FR-β can mediate internalization of folate-linked therapeutic agents into cells (*29*). A FR targeted imaging agent has been evaluated for tumor imaging in a human study (*30*). However, evaluation of ^{18}F-FOL uptake in human sarcoid lesions was not possible and therefore, a study with a tracer approved for clinical use will be needed to test feasibility of imaging FR-β in patients with sarcoidosis.

CONCLUSION

In a rat model of autoimmune myocarditis, ^{18}F-FOL PET specifically detects inflamed myocardium containing macrophages expressing FR-β, which are also present in human cardiac sarcoid lesions. Imaging of FR-β expression is a potential approach for the detection of active myocardial inflammation.

ACKNOWLEDGMENTS

The authors thank Aake Honkaniemi for assistance in PET studies, Marja-Riitta Kajaala and Erica Nyman (Histology Core, Institute of Biomedicine, University of Turku) for tissue sectioning and immunohistochemical staining and Timo Kattelus for assistance in Figure preparation.

DISCLOSURE

This study was conducted within the Finnish Centre of Excellence in Cardiovascular and Metabolic Diseases supported by the Academy of Finland, University of Turku, Turku University Hospital, and Åbo Akademi University. This study was financially supported by grants from the Academy of Finland, Business Finland, Jane and Aatos Erkko Foundation, Finnish Foundation for Cardiovascular Research, the Finnish Medical Foundation and Sigrid Jusélius Foundation. The authors declare that they have no competing interests.

KEY POINTS

QUESTION: Can folate receptor β (FR-β)–targeted imaging detect myocarditis?

PERTINENT FINDINGS: We evaluated whether ^{18}F-FOL, a positron emission tomography (PET) tracer targeting FR-β detects rat autoimmune myocarditis. Cardiac inflammatory lesions were detected histologically in 10 out of 18 (56%) immunized rats. PET shows specific ^{18}F-FOL uptake in inflamed myocardium containing FR-β-expressing macrophages (SUV_{mean}, 2.1 ± 1.1 vs. 0.4 ± 0.2 in non-inflamed myocardium; $P < 0.01$). FR-β expressing macrophages were found in human cardiac sarcoidosis specimens.

IMPLICATIONS FOR PATIENT CARE: Current imaging techniques have limited specificity for detecting myocardial inflammation. Imaging of FR-β-expression is a potential approach for specific detection of active myocardial inflammation.

REFERENCES

1. Caforio AL, Pankuweit S, Arbustini E, et al. Current state of knowledge on etiology, diagnosis, management, and therapy of myocarditis: a position statement of the European Society of Cardiology Working Group on Myocardial and Pericardial Diseases. *Eur Heart J*. 2013;34:2636-2648.
2. Kadkhodayan A, Chareonthaitawee P, Raman SV, Cooper LT. Imaging of inflammation in unexplained cardiomyopathy. *JACC Cardiovasc Imaging*. 2016;9:603-617.
3. Friedrich MG, Sechtem U, Schulz-Menger J, et al. Cardiovascular Magnetic Resonance in Myocarditis: A JACC White Paper. *J Am Coll Cardiol*. 2009;53:1475–1487.
4. Youssef G, Leung E, Mylonas I, et al. The use of ^{18}F-FDG PET in the diagnosis of cardiac sarcoidosis: a systematic review and metaanalysis including the Ontario experience. *J Nucl Med*. 2012;53:241-248.
5. Blankstein R, Osborne M, Naya M, et al. Cardiac positron emission tomography enhances prognostic assessments of patients with suspected cardiac sarcoidosis. *J Am Coll Cardiol*. 2014;63:329-336.
6. Tang R, Wang JT, Wang L, et al. Impact of patient preparation on the diagnostic performance of ^{18}F-FDG PET in cardiac sarcoidosis: A systematic review and meta-analysis. *Clin Nucl Med*. 2016;41:e327-339.
7. Maya Y, Werner RA, Schütz C, et al. ^{11}C-Methionine PET of myocardial inflammation in a rat model of experimental autoimmune myocarditis. *J Nucl Med*. 2016;57:1985–1990.
8. Martineau P, Pelletier-Galarneau M, Juneau D, et al. Imaging Cardiac Sarcoidosis With FLT-PET Compared With FDG/Perfusion-PET: A Prospective Pilot Study. *JACC Cardiovasc Imaging*. 2019;12:2280-2281.
9. Lapa C, Reiter T, Kircher M, et al. Somatostatin receptor based PET/CT in patients with the suspicion of cardiac sarcoidosis: an initial comparison to cardiac MRI. *Oncotarget*. 2016;7:77807-77814.

10. Gormsen LC, Haraldsen A, Kramer S, Dias AH, Kim WY, Borghammer P. A dual tracer ^{68}Ga-DOTANOC PET/CT and ^{18}F-FDG PET/CT pilot study for detection of cardiac sarcoidosis. *EJNMMI Res*. 2016;6:52.
11. Kim GR, Paeng JC, Jung JH, et al. Assessment of TSPO in a rat experimental autoimmune myocarditis model: A comparison study between [^{18}F]Fluoromethyl-PBR28 and [^{18}F]CB251. *Int J Mol Sci*. 2018;19:276.
12. Lapa C, Reiter T, Li X, et al. Imaging of myocardial inflammation with somatostatin receptor based PET/CT - A comparison to cardiac MRI. *Int J Cardiol*. 2015;194:44-49.
13. Paulos CM, Turk MJ, Breur GJ, Low PS. Folate receptor-mediated targeting of therapeutic and imaging agents to activated macrophages in rheumatoid arthritis. *Adv Drug Deliv Rev*. 2004;56:1205–1217.
14. Hu Y, Wang B, Shen J, et al. Depletion of activated macrophages with a folate receptor-beta-specific antibody improves symptoms in mouse models of rheumatoid arthritis. *Arthritis Res Ther*. 2019;21:143.
15. Silvola JMU, Li X, Virta J, et al. Aluminum fluoride-18 labeled folate enables in vivo detection of atherosclerotic plaque inflammation by positron emission tomography. *Sci Rep*. 2018;8:9720.
16. Ni NC, Jin CS, Cui L, et al. Non-invasive macrophage tracking using novel porphysome nanoparticles in the post-myocardial infarction murine heart. *Mol Imaging Biol*. 2016;18:557-568.
17. Kodama M, Matsumoto Y, Fujiwara M, Masani F, Izumi T, Shibata A. A novel experimental model of giant cell myocarditis induced in rats by immunization with cardiac myosin fraction. *Clin Immunol Immunopathol*. 1990;57:250–262.
18. Kamala T. Hock immunization: A humane alternative to mouse footpad injections. *J Immunol Methods*. 2007;328:204–214.
19. Ekström K, Lehtonen J, Nordenswan HK, et al. Sudden death in cardiac sarcoidosis: an analysis of nationwide clinical and cause-of-death registries. *Eur Heart J*. 2019;40:3121-3128
20. Shen J, Putt KS, Visscher DW, et al. Assessment of folate receptor-β expression in human neoplastic tissues. Oncotarget. 2015;6:14700–14709.

21. Ståhle M, Kytö V, Kiugel M, et al. Glucagon-like peptide-1 receptor expression after myocardial infarction: Imaging study using ^{68}Ga-NODAGA-exendin-4 positron emission tomography. *J Nucl Cardiol*. 2018. “Epub ahead of print”
22. Kiugel M, Dijkgraaf I, Kytö V, et al. Dimeric [^{68}Ga]DOTA-RGD peptide targeting αvβ 3 integrin reveals extracellular matrix alterations after myocardial infarction. *Mol Imaging Biol*. 2014;16:793-801.
23. Kodama M, Zhang S, Hanawa H, Shibata A. Immunohistochemical characterization of infiltrating mononuclear cells in the rat heart with experimental autoimmune giant cell myocarditis. *Clin Exp Immunol*. 1992;90:330-335.
24. Okura Y, Yamamoto T, Goto S, et al. Characterization of cytokine and iNOS mRNA expression in situ during the course of experimental autoimmune myocarditis in rats. *J Mol Cell Cardiol*. 1997;29:491-502.
25. Werner RA, Wakabayashi H, Bauer J, et al. Longitudinal ^{18}F-FDG PET imaging in a rat model of autoimmune myocarditis. *Eur Heart J Cardiovasc Imaging*. 2019;20:467-474.
26. van Heeswijk RB, De Blois J, Kania G, et al. Selective in vivo visualization of immune-cell infiltration in a mouse model of autoimmune myocarditis by fluorine-19 cardiac magnetic resonance. *Circ Cardiovasc Imaging*. 2013;6:277-284.
27. Lee S, Im HJ, Kang S, et al. Noninvasive imaging of myocardial inflammation in myocarditis using ^{68}Ga-tagged mannosylated human serum albumin positron emission tomography. *Theranostics*. 2017;7:413–424.
28. Bandara NA, Hansen MJ, Low PS. Effect of receptor occupancy on folate receptor internalization. *Mol Pharm*. 2014;11:1007-1013.
29. Xia W, Hilgenbrink AR, Matteson EL, Lockwood MB, Cheng JX, Low PS. A functional folate receptor is induced during macrophage activation and can be used to target drugs to activated macrophages. *Blood*. 2009;113:438-446.
30. Fisher RE, Siegel BA, Edell SL, et al. Exploratory study of ^{99m}Tc-EC20 imaging for identifying patients with folate receptor–positive solid tumors. *J Nucl Med*. 2008;49:899–906.

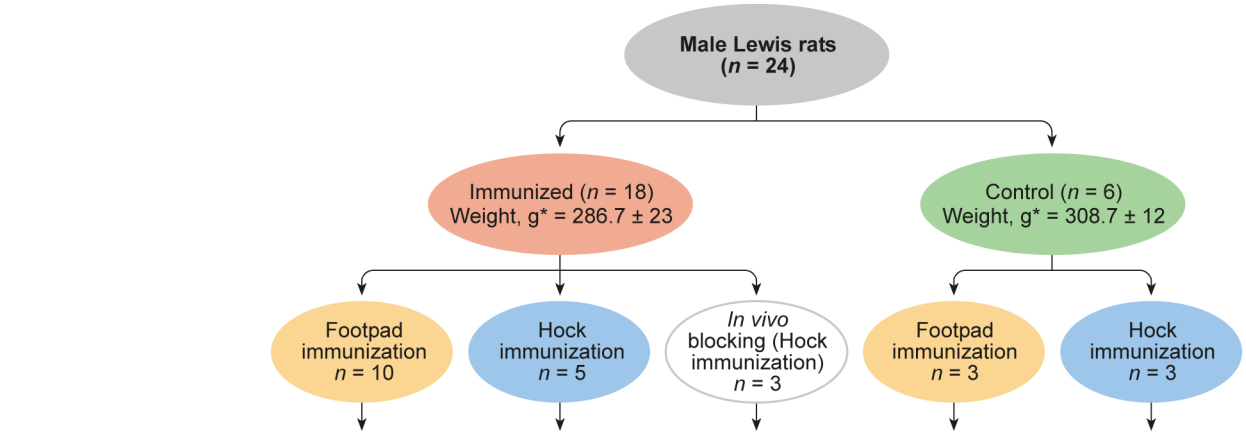

In vivo ^{18}F-FOL PET/CT	13**	5	3	3	3
In vivo ^{18}F-FDG PET/CT	10	0	0	3	0
Rats with histologically proven inflammatory lesions in myocardium	4	3	3	0	0
Ex vivo ^{18}F-FOL gamma counting	4	3	0	3	3
Ex vivo ^{18}F-FOL autoradiography	4	3	3	3	3
In vitro autoradiography	3	0	0	0	0

FIGURE 1. A flow diagram of the study design and numbers of animals used. Blocking study = *in vivo* competition assay with 100-fold molar excess of folate glucosamine injected 10 min before ^{18}F-FOL. n = number. *Values are mean ± SD. **10 had a static scan and all others a dynamic scan.

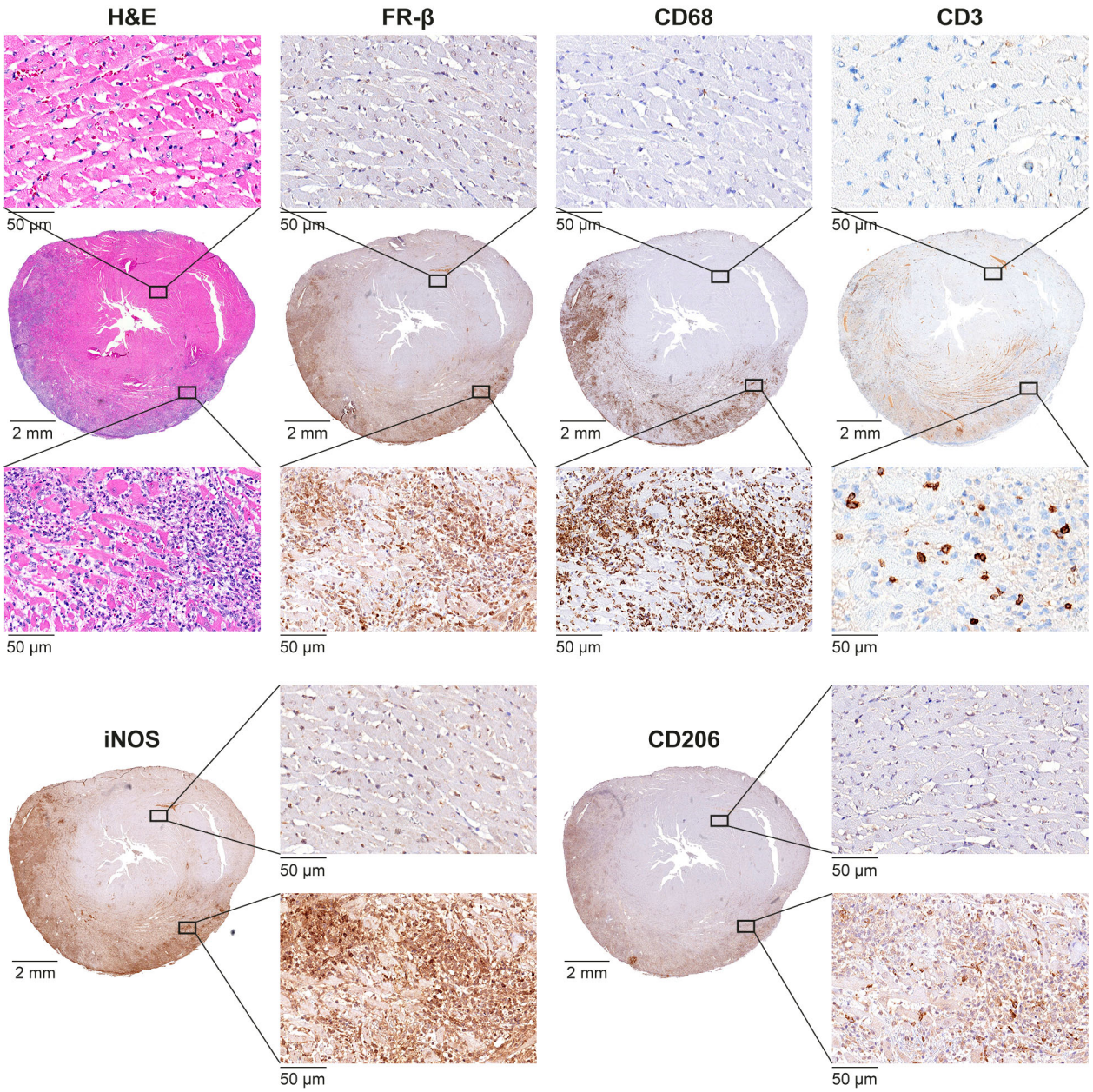

FIGURE 2. An inflammatory myocardial lesion in a rat with autoimmune myocarditis identified by hematoxylin and eosin (H&E) staining and stained with an antibody against folate receptor β (FR-β), which is co-localized with CD68-positive macrophages stained with an antibody against CD68. Scattered CD3 positive lymphocytes are also present. Staining with antibodies against inducible nitric oxide synthase (iNOS) indicates the presence of M1-polarized macrophages, and to a lesser extent the presence of M2-polarized macrophages stained with antibodies against CD206.

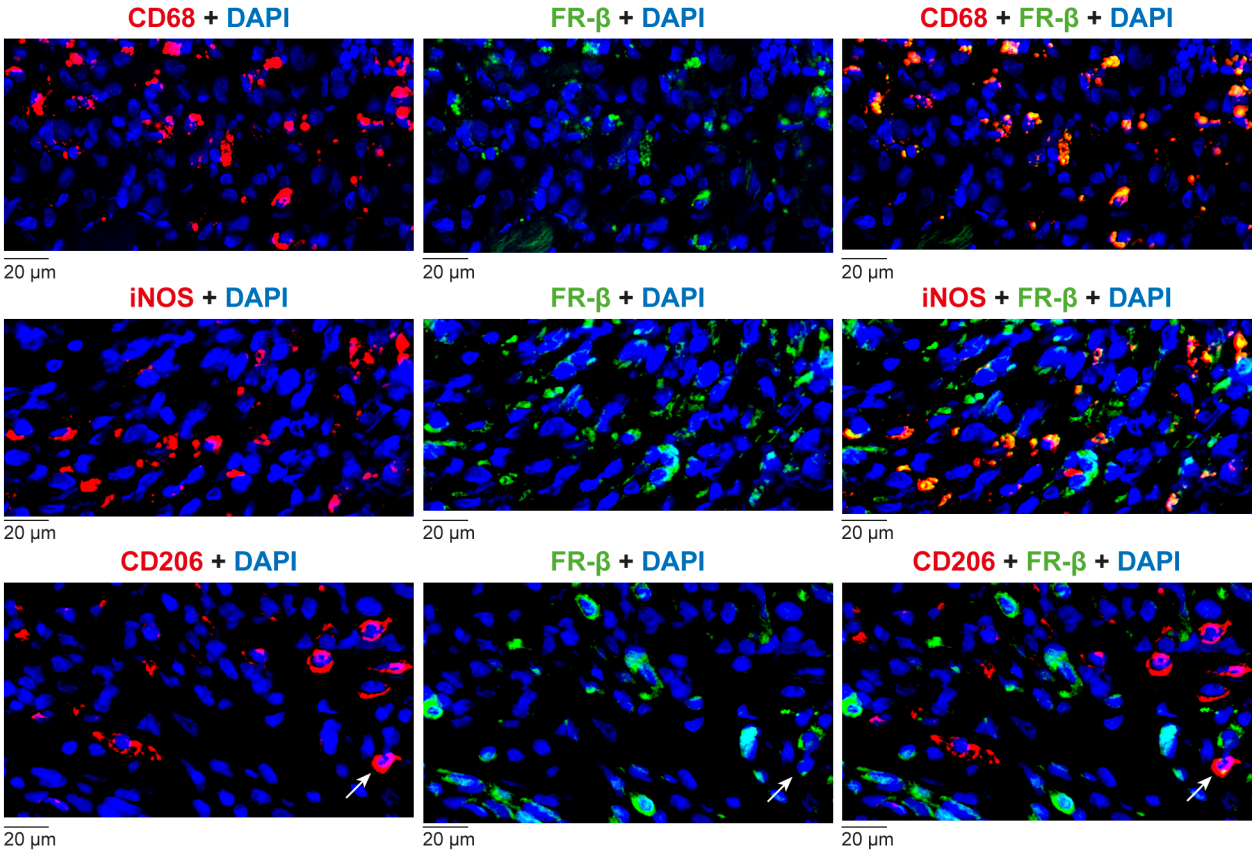

FIGURE 3. Localization of folate receptor β (FR-β) in rat autoimmune myocarditis. Double immunofluorescence staining of sections of an inflamed myocardial lesion from an immunized rat heart show CD68-positive macrophages, M1-polarized macrophages (iNOS), M2-polarized macrophages (CD206; red, left panels), and FR-β (green, middle panels). Note the co-localization of FR-β with CD68-positive macrophages, and the co-localization of M1-polarized macrophages (yellow, right panels) and an M2-polarized macrophage (white arrows).

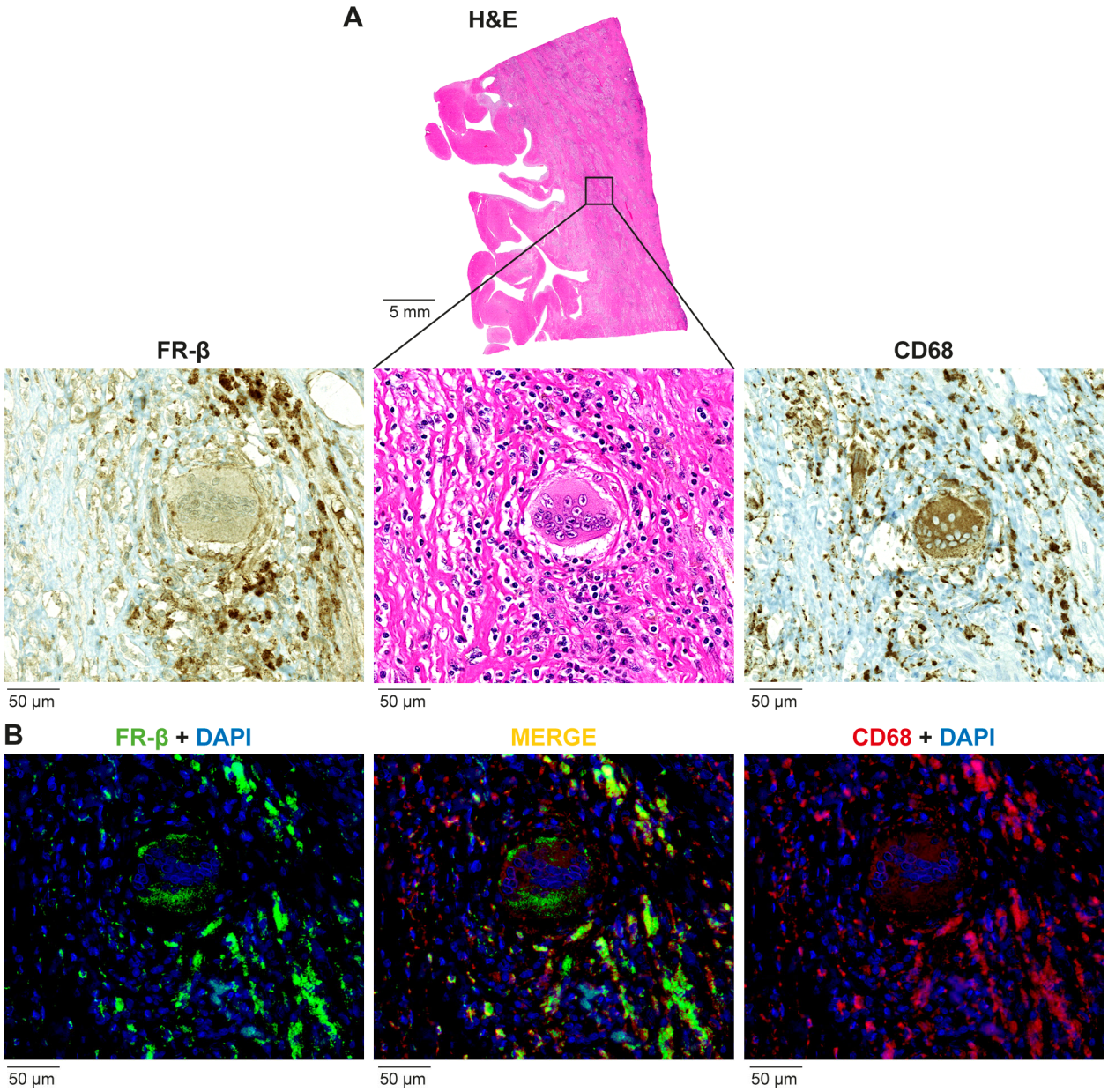

FIGURE 4. Folate receptor β (FR-β) in a human cardiac sarcoid lesion. (**A**) An inflammatory lesion identified by hematoxylin and eosin (H&E) staining and stained with antibodies against CD68 positive macrophages (CD68) and folate receptor β (FR-β). (**B**) Double immunofluorescence staining with antibodies against CD68-positive macrophages, (red, right panel) and FR-β (green, left panel) shows co-localization of FR-β with CD68-positive macrophages (yellow, middle panel).

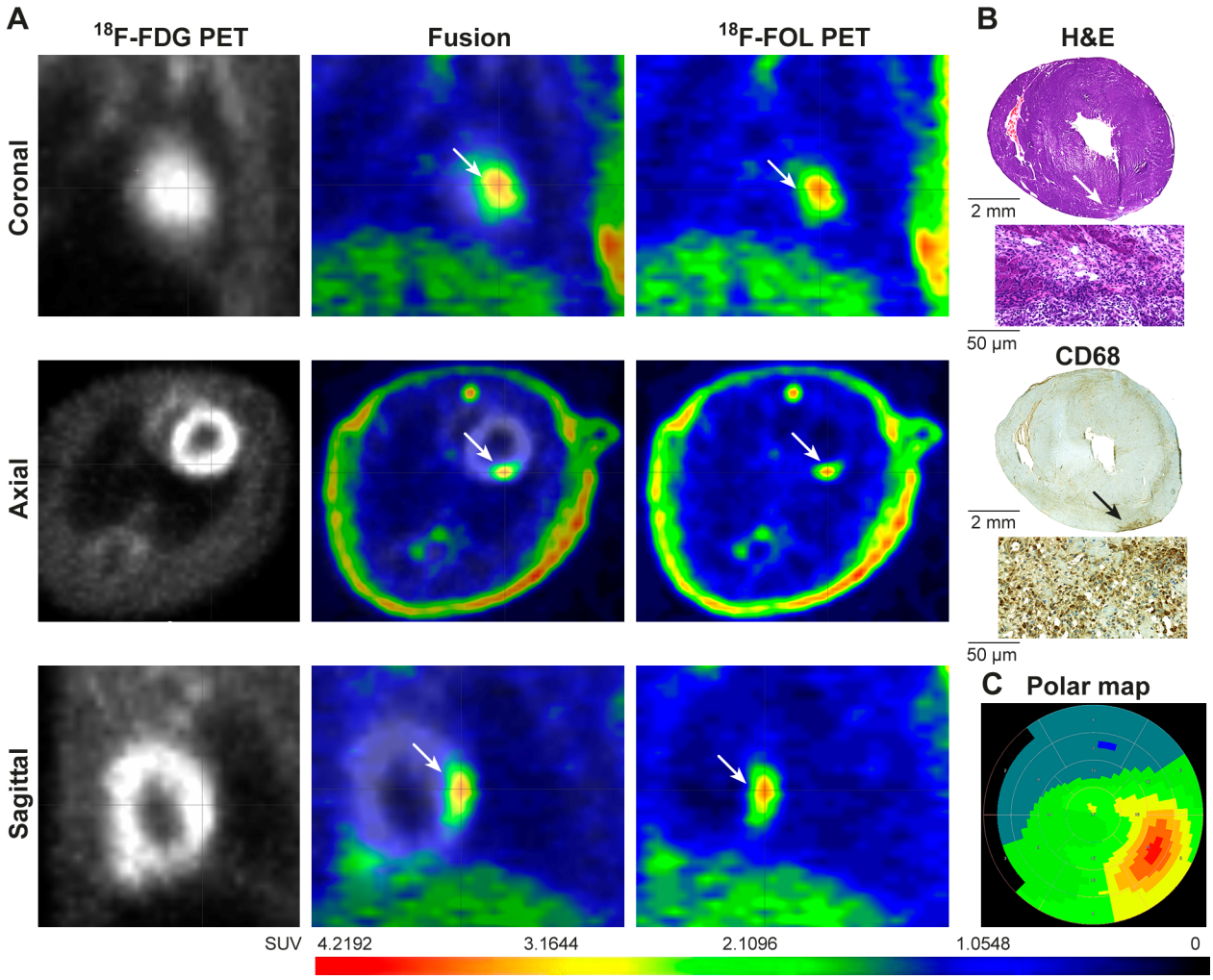

FIGURE 5. (**A**) *In vivo* PET images with ^{18}F-FDG and ^{18}F-FOL tracers in a rat with autoimmune myocarditis. PET images at 30-40 min show focal ^{18}F-FOL uptake (white arrows) in the posterior left ventricle (LV) wall. (**B**) Uptake is co-localized with an inflamed myocardial lesion in the posterior wall of the LV, as shown in the histological sections stained with hematoxylin and eosin (H&E) or antibodies against CD68 (macrophages). (**C**) A polar map demonstrates ^{18}F-FOL uptake in the posterior wall. ^{18}F-FOL uptake is low elsewhere in the LV myocardium.

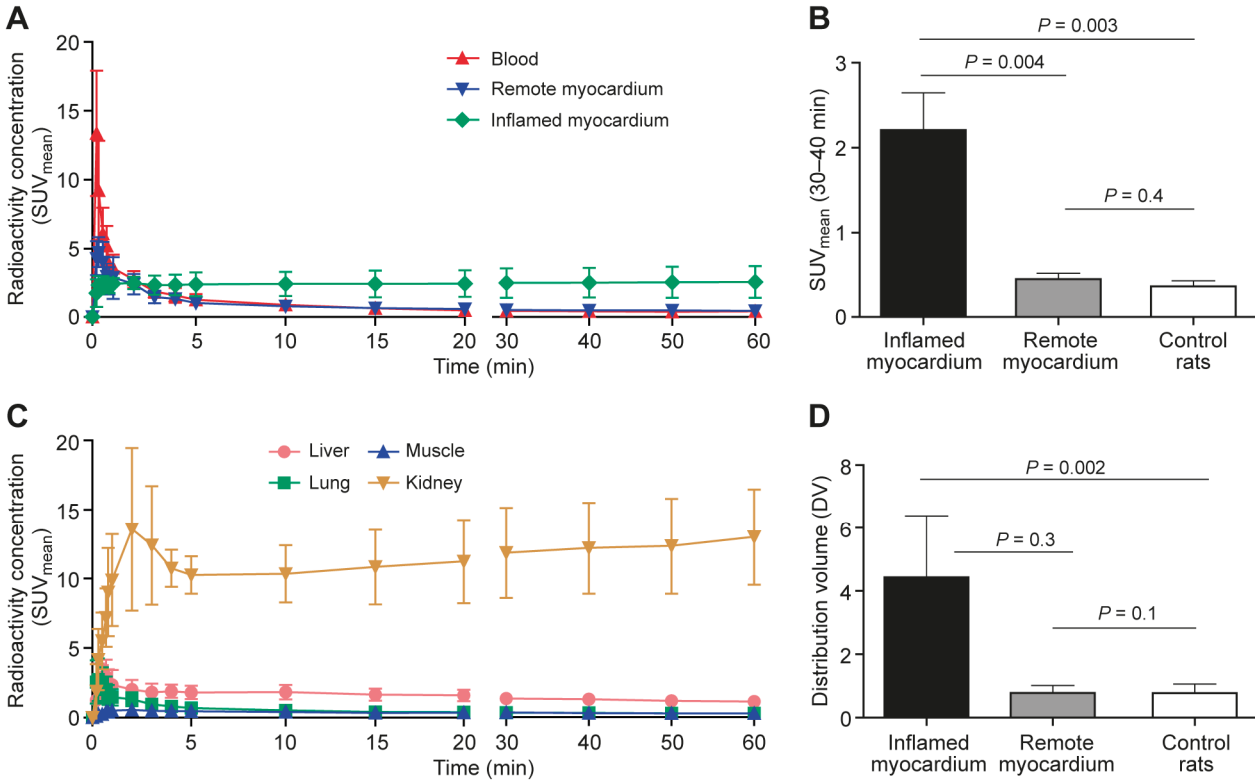

FIGURE 6. PET imaging of ^{18}F-FOL uptake. Time-activity curves (**A** and **C**) from rats with autoimmune myocarditis (n = 4) show that ^{18}F-FOL uptake (mean standardized uptake value, SUV_{mean}) remains higher in inflamed myocardium than in remote non-inflamed myocardium or blood (inferior vena cava). Bars indicate standard deviation. (**B**) The average myocardial ^{18}F-FOL uptake (SUV_{mean}) 30–40 min after injection is higher in the inflamed myocardium (n = 7) than in the remote myocardium of immunized rats (n = 7) or in the myocardium of control rats (n = 6). (**D**) The distribution volume indicating irreversible uptake of ^{18}F-FOL is also increased in the inflamed myocardium (n = 4) in comparison with the remote myocardium of immunized rats (n = 4) or the myocardium of control rats (n = 6). Values are mean ± SD; unpaired t-tests for comparisons of inflamed and control myocardium, and paired t-tests for comparisons of inflamed and remote myocardium.

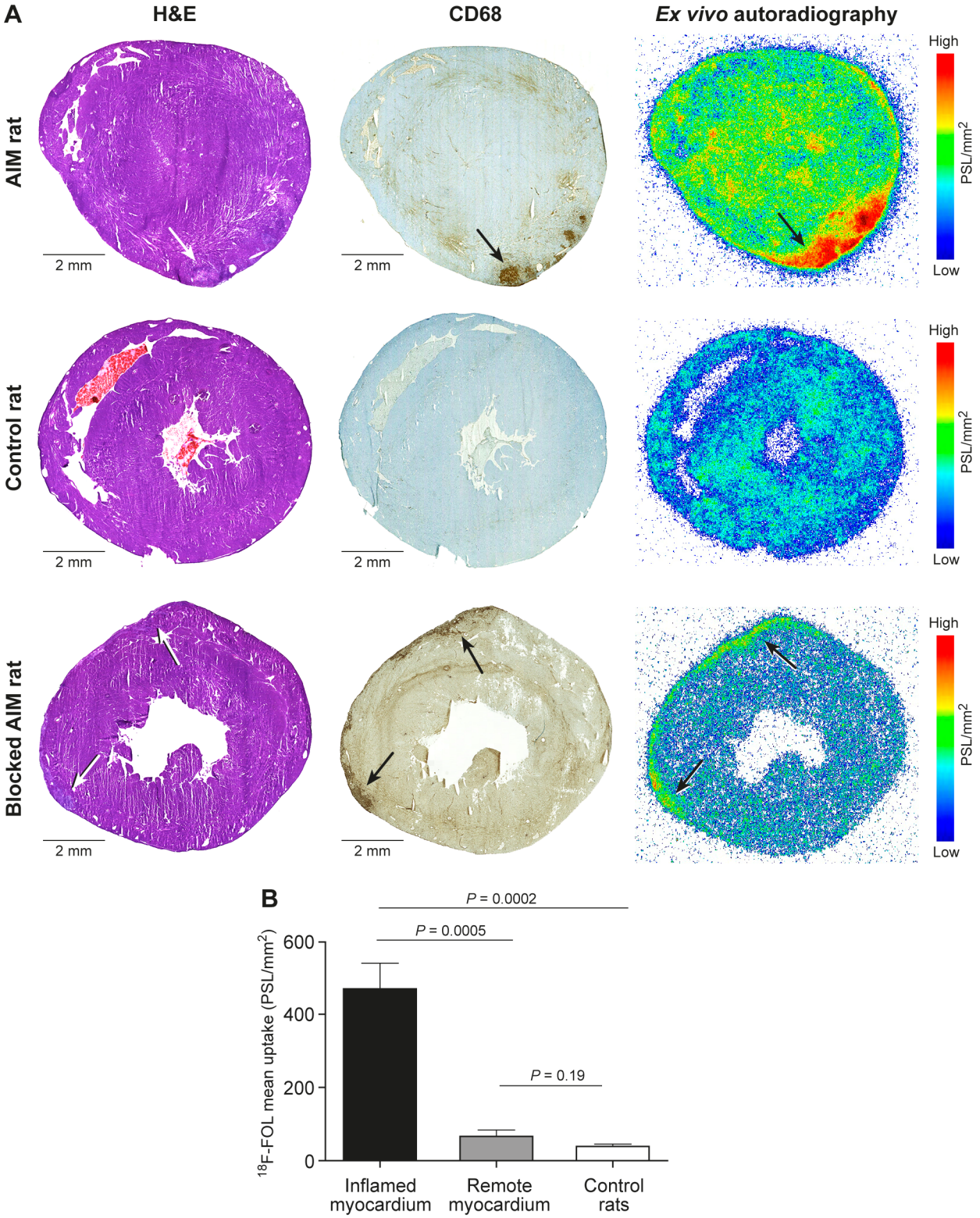

FIGURE 7. *Ex vivo* autoradiography of ^{18}F-FOL uptake. Representative left ventricular short axis sections stained with hematoxylin and eosin (H&E) or antibodies against CD68 on macrophages in a rat with

autoimmune myocarditis (AIM), a control rat and an AIM rat after co-injection with a 100-fold excess of unlabeled FR-β ligand folate glucosamine. Ex vivo autoradiography shows ^{18}F-FOL uptake co-localized with inflammatory lesions (black arrows), which is reduced by blocking agent. (**B**) Bars demonstrate ^{18}F-FOL uptake by *ex vivo* autoradiography as mean photo-stimulated luminescence per square millimeter (PSL/mm^2) in inflamed myocardium (n = 7), remote myocardium of immunized rats (n = 7), and myocardium of control rats (n = 6). Values are mean ± SD; unpaired t-tests for comparisons of inflamed and control myocardium, and paired t-tests for comparisons of inflamed and remote myocardium.

SUPPLEMENTAL MATERIAL

Folate Receptor β Targeted PET Imaging of Macrophages in Autoimmune Myocarditis

Supplemental Table 1. Primary antibodies used for immunohistochemical and immunofluorescence staining

Antibody	Catalogue number	Dilution		Manufacturer
		Cryo	Paraffin	
Rat sections *(Immunohistochemistry)*				
FR-β	Polyclonal rabbit anti-rat FR-β, orb317614		1:200	Biorbyt, Cambridge, UK
CD68	Monoclonal mouse anti-rat CD68, MCA341R	1:1000		AbD Serotec, Munich, Germany
CD68	Monoclonal mouse anti-rat CD68, MCA341GA		1:2000	AbD Serotec, Munich, Germany
iNOS	Polyclonal rabbit anti-rat iNOS, ab15323		1:350	Abcam, Cambridge, UK
CD206	Polyclonal rabbit anti-rat anti-mannose receptor, ab64693		1:5000	Abcam, Cambridge, UK
CD3	Monoclonal rabbit anti-rat CD3, 2GV6		1:1	Ventana, Arizona, USA
Rat sections *(Immunofluorescence)*				
FR-β	Biotinylated monoclonal anti-human FR-β, m909	1:50		Non-commercial (*21,23*)
Streptavidin	Alexa Fluor™ 488 conjugate S32354	1:200		Thermo Fisher, Massachusetts, USA
CD68	Monoclonal mouse anti-rat CD68, MCA341R	1:1000		AbD Serotec, Munich, Germany
iNOS	Polyclonal rabbit anti-rat iNOS, ab15323	1:1000		Abcam, Cambridge, UK
CD206	Polyclonal rabbit anti-rat anti-mannose receptor, ab64693	1:1000		Abcam, Cambridge, UK
Human tissue sections *(Immunohistochemistry)*				
FR-β	Polyclonal rabbit anti-rat FR-β, orb317614		1:200	Biorbyt, Cambridge, UK
CD68	Monoclonal Mouse Anti-Human CD68, M0876		1:200	Dako, Agilent Technologies Inc., California, USA
Human tissue sections *(Immunofluorescence)*				
FR-β	Biotinylated monoclonal anti-human FR-β, m909		1:50	Non-commercial (*21*)
Streptavidin	Alexa Fluor™ 488 conjugate S32354		1:200	Thermo Fisher, Massachusetts, USA
CD68	Monoclonal Mouse Anti-Human CD68, M0876		1:200	Dako, Agilent Technologies Inc., California, USA

Supplemental Table 2. Kinetic modeling of ^{18}F-FOL uptake

Study region	**DV**	**Ki**	**K1**
Inflamed myocardium	4.0 ± 1.7	0.03 ± 0.02	0.2 ± 0.02
Remote myocardium	0.7 ± 0.2	0.003 ± 0.001	0.04 ± 0.02
Control rats	0.8 ± 0.2	0.004 ± 0.002	0.03 ± 0.01
***P*-values**			
Inflamed myocardium vs. Remote	0.04	0.04	0.000004
Inflamed myocardium vs. Control	0.003	0.003	0.001
Remote vs. Control	0.1	0.4	0.1

Results are expressed as mean ± SD with the probability value (*P*) from a Student's *t*-test. DV = distribution volume, Ki = net influx rate, K1 = plasma-to-tissue transport rate compartmental model value.

Supplemental Table 3. *Ex vivo* biodistribution* of ^{18}F-FOL in seven immunized rats and six control rats at 100 min after intravenous injection

	Immunized rats	**Control rats**	***P*-value**
Blood	0.07 ± 0.01	0.08 ± 0.04	0.53
Bone marrow	3.9 ± 1.63	2.92 ± 1.16	0.27
Heart	1.15 ± 0.54	0.39 ± 0.07	0.01*
Intestine without content	1.69 ± 0.37	1.35 ± 0.34	0.14
Kidney	36.56 ± 24.08	26.46 ± 24.86	0.51
Liver	1.48 ± 0.72	0.73 ± 0.31	0.053
Lung	0.73 ± 0.16	0.41 ± 0.15	0.01*
Lymph node	4.65 ± 1.06	3.20 ± 1.58	0.10
Muscle	0.36 ± 0.07	0.29 ± 0.08	0.17
Plasma	0.12 ± 0.02	0.16 ± 0.05	0.86
Pancreas	0.83 ± 0.28	0.57 ± 0.09	0.07
Spleen	4.08 ± 2.80	1.86 ± 0.99	0.12
Thymus	2.45 ± 1.35	0.79 ± 0.21	0.02*
Urine	39.68 ± 27.22	46.37 ± 34.69	0.73
White adipose tissue	0.39 ± 0.13	0.23 ± 0.05	0.02*

The results are expressed as SUVs (mean ± SD).

*A statistically significant difference based on Student's *t*-test.

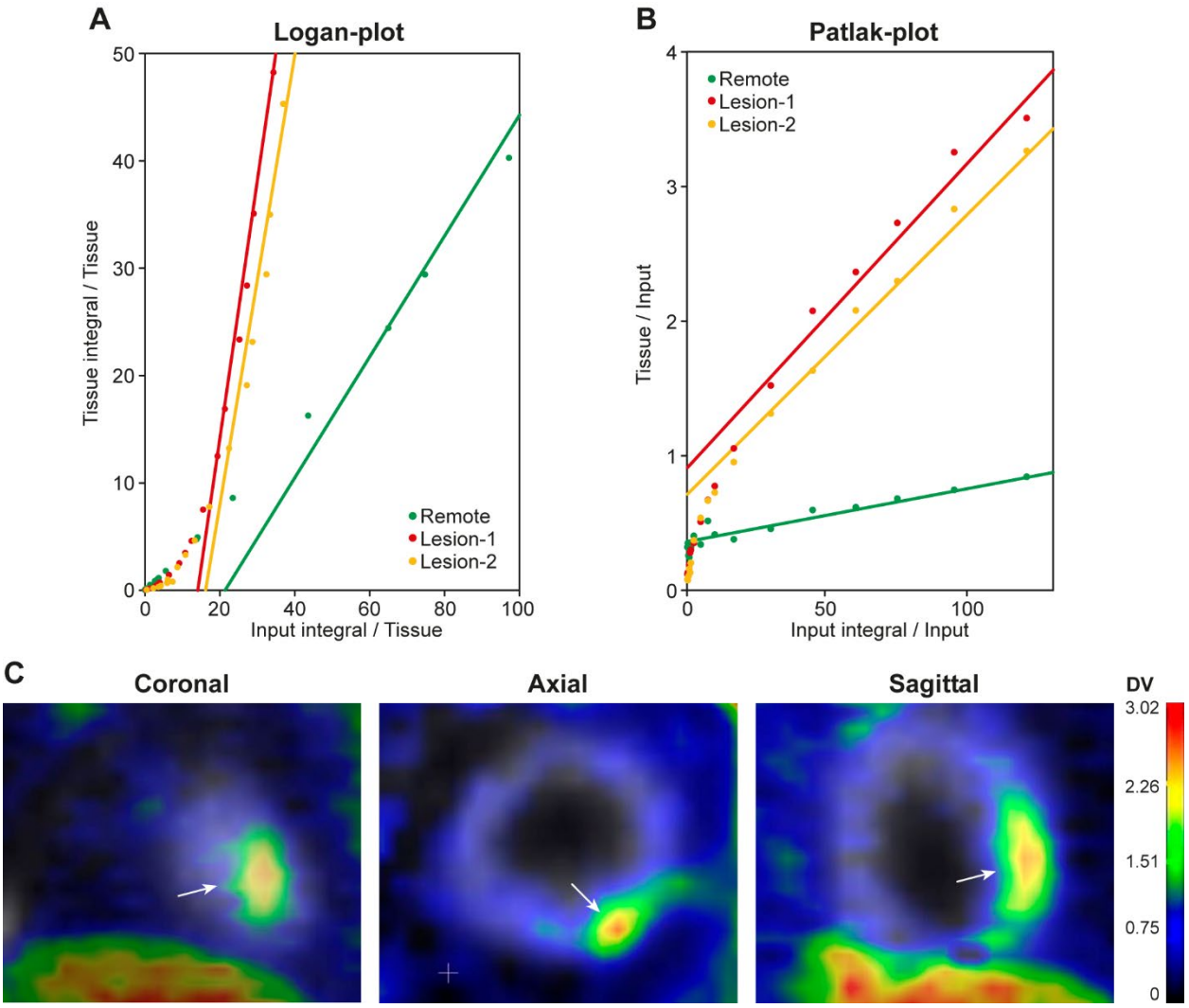

Supplemental Figure 1. (**A**) Representative Logan plot of an immunized rat with two inflammatory lesions in the myocardium of left ventricle (LV) at 5–60 min post-injection, indicating reversible receptor binding of ^{18}F-FOL. (**B**) Representative Patlak plot of the same immunized rat at 5–60 min post-injection, indicating irreversible receptor binding of ^{18}F-FOL. (**C**) DV-generated positron emission tomography (PET) images with ^{18}F-FOL fused with ^{18}F-FDG PET (grey scale) images showing clear and focal ^{18}F-FOL uptake in an inflammatory lesion in the myocardium of the posterior LV wall of a rat with autoimmune myocarditis (white arrows). Metabolite-corrected plasma time-activity curves were used as input functions. Image-derived blood curves measured in the vena cava and LV cavity were converted into metabolite-corrected plasma curves using the group median plasma-to-blood ratio and percent of ^{18}F-FOL measured in the metabolite analysis. DV and Ki were calculated as the slope of the plot 5–60 min after tracer injection. Parametric images of DV were obtained using Logan plots and modeling images, and the data were compared with standardized uptake values.

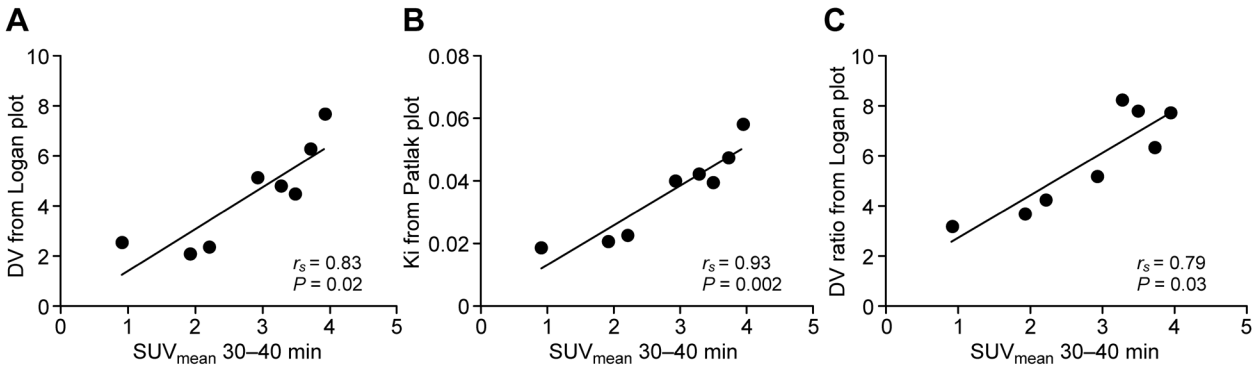

Supplemental Figure 2. (**A**) Correlation* between mean standardized uptake value (SUV_{mean}) on PET 30–40 min after ^{18}F-FOL injection and the distribution volume (DV) derived from the Logan plot in myocardial inflammatory lesions (*n* = 8) in four immunized rats. (**B**) Correlation between SUV_{mean} on PET 30–40 min after ^{18}F-FOL injection and net influx rate (Ki) derived from a Patlak plot in myocardial inflammatory lesions (*n* = 8) in four immunized rats. (**C**) Correlation between SUV_{mean} on PET 30–40 min after ^{18}F-FOL injection, and the ratio of DV in inflammatory lesions (*n* = 8) to remote myocardium in four immunized rats. *Spearman's test (r_s) was used to analyze correlation between two continuous variables.

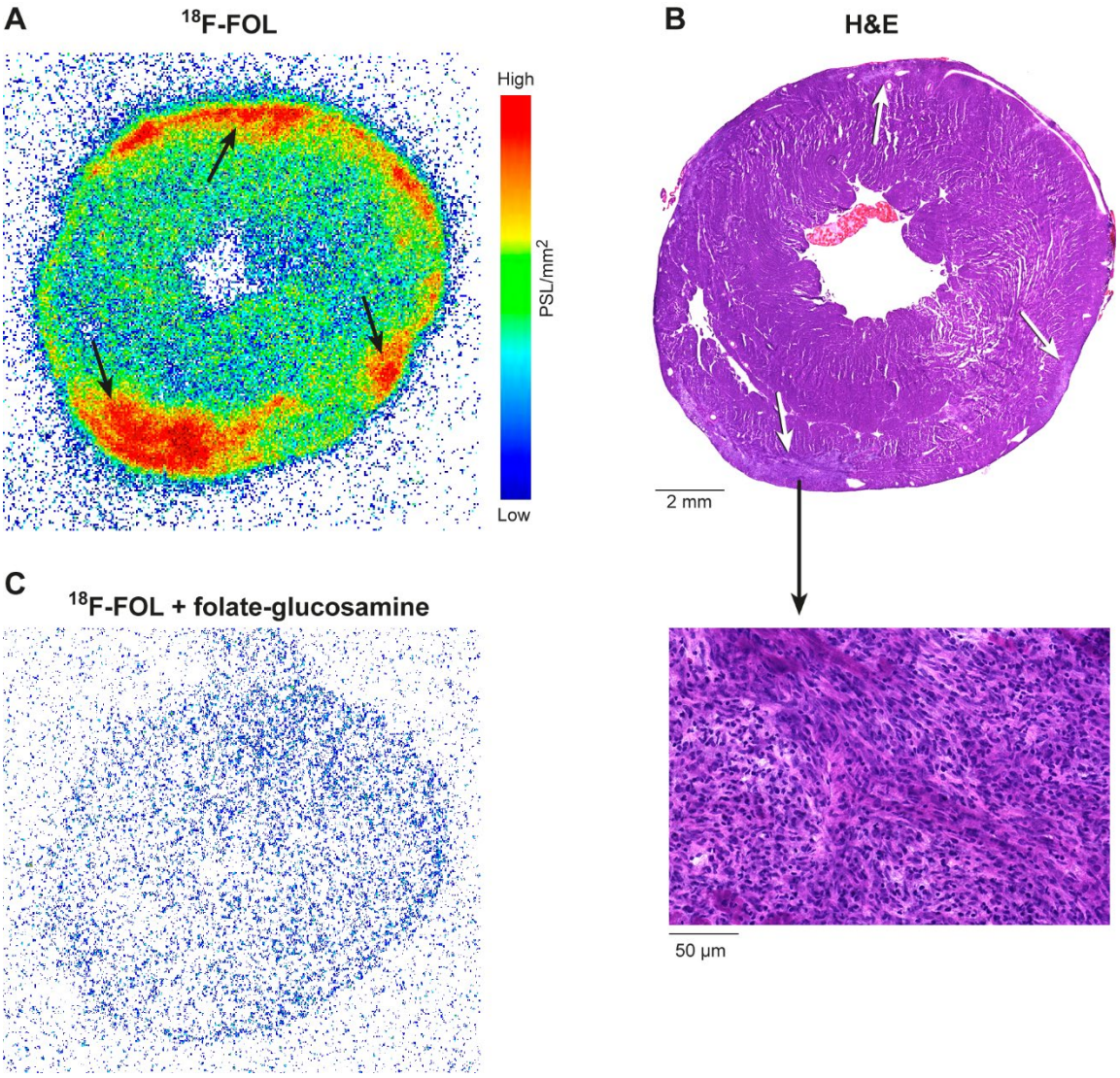

Supplemental Figure 3. (**A**) Autoradiography demonstrates *in vitro* binding of ^{18}F-FOL (black arrows) in a rat myocardial tissue section containing inflamed lesions shown by hematoxylin and eosin (H&E) staining (red arrows in **B**). (**C**) In an adjacent tissue section, co-incubation with folate glucosamine reduced ^{18}F-FOL binding. PSL/mm^2 = photo-stimulated luminescence per square millimeter.